PROCEEDINGS OF SCIENCE

The BATSE 5B Spectral Catalog and the 2-Year *Fermi*/GBM Spectral Catalog

Adam Goldstein*
University of Alabama in Huntsville
E-mail: adam.m.goldstein@nasa.gov

Robert D. Preece
University of Alabama in Huntsville
E-mail: rob.preece@nasa.gov

J. Michael Burgess
University of Alabama in Huntsville
E-mail: james.m.burgess@nasa.gov

We present the final and complete BATSE 5B spectral catalog of over 2000 Gamma-Ray Bursts. We emphasize the E_{peak} distributions of this complete set of data, as well as the possibility of a cosmologically-independent classifier for GRBs. In addition, we present a first look at the global spectral properties of GRBs detected during the first two years of operation of the Fermi/GBM and discuss the similarities and differences between this sample and the BATSE 5B spectral catalog. A preliminary interpretation of the results will be provided, as well as a discussion on what is to be expected for the continuing research.

8th INTEGRAL Workshop, "The Restless Gamma-ray Universe"
September 27-30, 2010
Dublin, Ireland

*Speaker.

PoS(INTEGRAL 2010)094

1. Introduction

The newly complete and final BATSE 5B Spectral Catalog (Goldstein et al., in prep.) and the first 2-Year GBM Catalog (Goldstein et al., in prep.) are expected to yield a wealth of information regarding the bulk spectral properties of gamma-ray bursts. The complete BATSE catalog is comprised of 2,141 GRBs resulting in 19,936 model spectra, while the first GBM catalog contains 3,867 spectra of 487 GRBs. Two sets of model spectra were fit to each GRB: a 3.5 sigma signal-to-noise selection for the duration of the burst (fluence spectra), and a peak count rate selection (peak flux spectra). For the BATSE catalog the peak count rate was measured over a 2 s time interval, while the GBM catalog contains peak selections of duration 1 s for long bursts and 64 ms for short bursts based on the T_{90} estimation for each burst. For the 5B Catalog, five models were fit to each of these spectra: a Band function, a power law with an exponential cutoff (Comptonized), a $\log_{10}$ Gaussian, a simple power law, and a smoothly broken power law. The same analysis was performed for GBM GRBs, but the $\log_{10}$ Gaussian was omitted in the GBM catalog.

2. Catalog Results

We present results primarily from the fluence spectra of both catalogs. The plotted histograms in Figure 1 show the distribution of E_{peak} and E_{break}, and Figure 2 shows distribution of power law indices from the catalog. The distributions include a goodness-of-fit cut requiring that the model fit be within the 3-sigma confidence interval. A 40% error cut on the 1-sigma errors was made on the E_{peak} and E_{break} distributions, and only those spectral indices which had a 1-sigma error of 0.3 or less were retained in their respective distributions. The histograms were normalized to the total number of fits in each set to enable the comparison between the two catalogs. As can

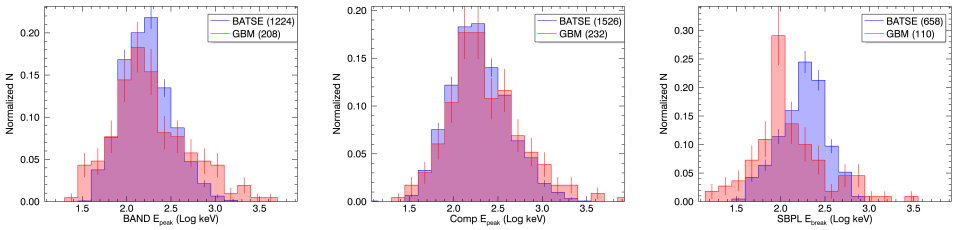

(a) Band E_{peak} (b) Comp E_{peak} (c) SBPL E_{break}

Figure 1: Histograms of the E_{peak} and E_{break} parameters. The histograms are normalized to allow comparison between BATSE and GBM. A distinction between the two datasets is the higher-energy tail in the GBM distribution of E_{peak}.

be seen in Figure 1, the BATSE E_{peak} and E_{break} distributions are centered about 200 keV, and are constrained within the full BATSE energy band (20 keV - 2 MeV). The GBM E_{peak} distributions are concentrated in the same energy range, but contain E_{peak} values previously unsampled by BATSE. The lower energy concentration in the Band E_{peak} distribution and the high energy tail in both the Band and Comptonized E_{peak} values can be attributed to the much larger energy range of GBM (8 keV - 40 MeV). This energy range allows the successful measure of short hard bursts with E_{peak}

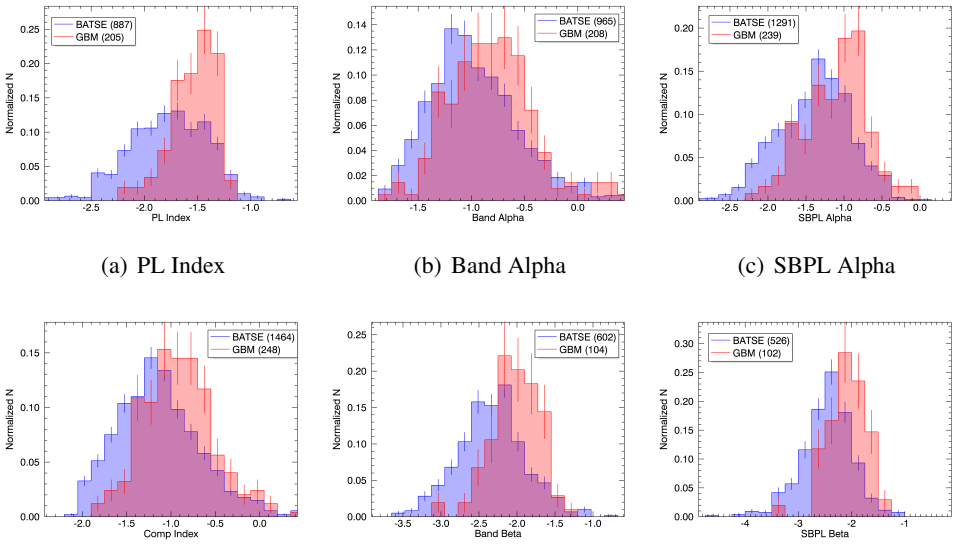

(a) PL Index (b) Band Alpha (c) SBPL Alpha

(d) Comp Index (e) Band Beta (f) SBPL Beta

Figure 2: Distributions of spectral indices. Notable difference between BATSE and GBM include the difference in the power law index distribution and the high-energy power law of the Band function: both BATSE distributions are wider and have steeper slopes on average.

values greater than 1 MeV. The GBM E_{break} distribution is shifted to lower energies, centered about 100 keV, which may also be an artifact of detector spectral coverage.

The low energy spectral index distributions of the Band and Comptonized functions, shown in Figures 2(a)–2(d), are consistent with a -1.0 power law index, and the Smoothly Broken Power Law index shifts from -1.3 to about -1.0 from the BATSE catalog to the GBM catalog. The power law index distribution for GBM is much more constrained than that for BATSE at an index of -1.5, and the BATSE power law index is widely distributed between -1.25 and -2.25. From Figures 2(e) & 2(f), high energy spectral index from the Band function is steeper, at -2.0 for GBM and about -2.5 for BATSE, and the index for the Smoothly Broken Power Law is shifted to a shallower index in the GBM catalog than in the BATSE catalog. It should be noted that E_{peak} can be derived for the Smoothly Broken Power Law, but only for a high energy index steeper than -2.0, which implies that many fewer GBM bursts can have a derived SBPL E_{peak} than is possible for the BATSE catalog.

3. Distributions

By using the chi-square goodness-of-fit statistic for each model fit, we can estimate the best model from the catalogs for each burst. We take a change in chi-square of 6 per degree of freedom to be significant, and we find that in both catalogs the Comptonized function is most preferred in more than half of all GRBs. In Figure 3, we present the best fit E_{peak} values from the fluence spectral fits and the peak flux spectral fits. It should be noted that many of the GRBs with E_{peak} greater than 1 MeV are short hard bursts, and the peak flux E_{peak} was measured on a 64 ms timescale compared to the 2 s timescale for BATSE GRBs.

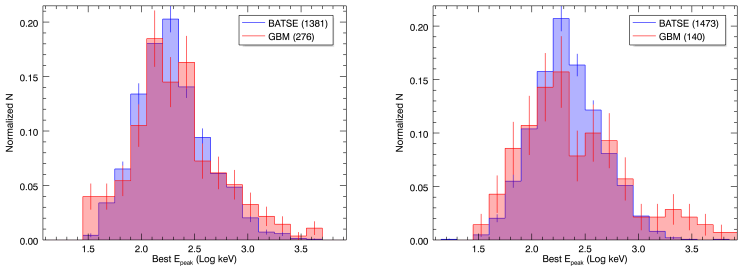

(a) Best Fluence E_{peak} (b) Best Peak Flux E_{peak}

Figure 3: Histogram of the best fluence and peak flux E_{peak}. Note the high-energy tail, particularly in (b) for GBM. This is likely due to the sensitivity of GBM to higher energies.

Using the best model fit for each burst, we can estimate the best derived photon flux and energy flux for each GRB. These are obviously quantities dependent on the energy range and sensitivity of the detectors, but give insight into the selection effects involved in GRB detection. Shown in Figure 4, the threshold for detection in BATSE is about 0.1 photon/s-cm^2 (3×10^{-8} erg/s-cm^2), while the threshold for GBM is about 0.8 photon/s-cm^2 (8×10^{-8} erg/s-cm^2). This is mainly due to the much smaller ($\sim 1/8$) total effective area of the GBM detectors compared to the BATSE Large Area Detectors, however, GBM has a better higher energy response and broader spectral coverage allowing for a more accurate modeling of the photon spectrum above a few hundred keV. This is shown by the large percentage of bursts with flux out to 30 photon/s-cm^2 (1.6×10^{-5} erg/s-cm^2).

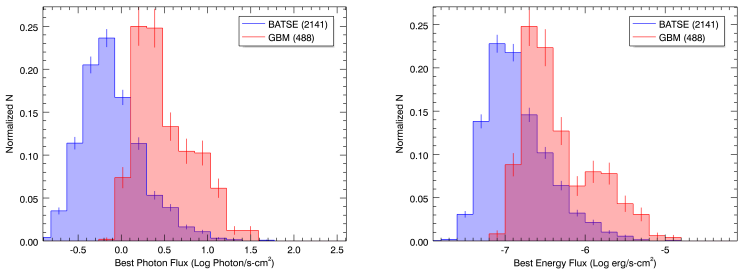

(a) Best Photon FluxE_{peak} (b) Best Energy Flux E_{peak}

Figure 4: The best model photon and energy flux distributions. These distributions are consistent with the difference in detector surface area between the two instruments.

4. Energy Ratio

Interesting discoveries have already been uncovered with these datasets and many more are expected. One such recent discovery is that of a new discriminator between two types of bursts, the E_{peak}/Fluence energy ratio [1]. This ratio provides a measure of spectral hardness similar to that found by Kouveliotou et al. (1993)[2], but it is independent of redshift in energy and is directly

related to the luminosity distance. Plotted in Figure 5 are the initial distributions from the 5B catalog and the results from the GBM catalog. The BATSE plot shows the distribution separated into long bursts (white) and short bursts (gray), and at least a marginal correlation has been found between the energy ratio and the T_{90} duration estimate of bursts.

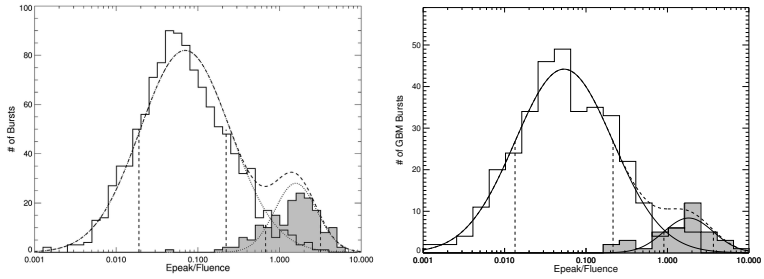

(a) BATSE Energy Ratio (b) GBM Energy Ratio

Figure 5: The Energy Ratio for BATSE and GBM. The split and overlap of the distributions are similar between the two instruments, as well as the peaks of the bimodal distributions. The white distribution is composed of long GRBs and the gray distribution comprises short GRBs.

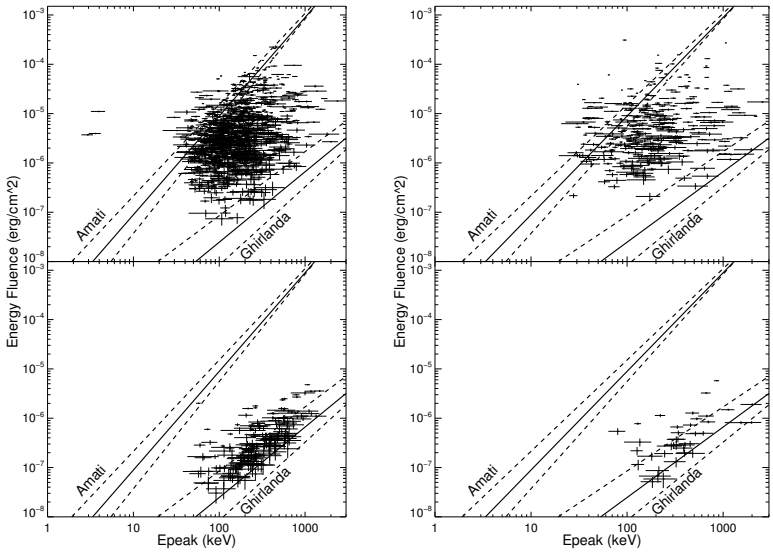

(a) BATSE E_{peak} vs. Fluence (b) GBM E_{peak} vs. Fluence

Figure 6: Plots of BATSE and GBM bursts in the E_{peak}-Fluence plane. Long GRBs inhabit the top frame of both plots, and the lower frames show the short GRBs. There is a clear distinction in the way both classes distribute, and may give a clue to the energetics involved. The short GRBs distribute close to the Ghirlanda lower limit line, which assumes a jet opening angle of 90 degrees. This indicates that short GRBs are much less collimated than most of long GRBs.

In addition, we investigate a method [3, 4] to determine the violation of the Amati [5] and Ghirlanda [6] relations with bursts of no known redshift. Plotting the lower limits of the relations

in the E_{peak}-Fluence (Figure 6) plane, we find that very few BATSE bursts can follow the Amati relation, although all BATSE bursts and most GBM bursts may be valid for the Ghirlanda relation. More importantly, below, we plot the long and short bursts separately for BATSE, we find that most long bursts are clustered between the Amati and Ghirlanda lower limits, while most of the short bursts are linearly dispersed along the Ghirlanda lower limit. A similar situation is observed with GBM bursts. This assumes a beaming factor of unity for the Ghirlanda relation, that is we assume the opening jet angle is 90 degrees. Interestingly, if we decrease the beaming factor (and thus the opening jet angle), the Ghirlanda lower limit moves towards the bulk of long bursts, and eventually all short bursts will violate the Ghirlanda lower limit. This appears to support findings that long bursts have a dispersion of small jet angles on the order of 2-12 degrees [7, 8] and short bursts have opening jet angles of about 90 degrees, as is supported by Watson et al. (2006)[9].

5. Conclusion

Close inspection of the bulk spectral properties of GRBs can lead to improvements in understanding of the physics of these immense explosions. Results may be skewed by detector selection effects, therefore it is advantageous to compare the spectral properties obtained by different instruments to ascertain the true distributions and correlations discovered in burst data. We anticipate that the catalogs will contribute much to the understanding of the spectral properties of GRBs. Already we have shown that another fundamental discriminator between classes of bursts can be defined, and there appears to be a method to calculating the jet opening angle from only the prompt gamma-ray emission. These findings could lead to the advancement of knowledge of GRBs, and the use of GRBs for other astrophysical studies, such as the study of dark matter and cosmology.

References

[1] A. Goldstein, R. D. Preece, & M. S. Briggs, *ApJ* **721** (2010) 1329.

[2] C. Kouveliotou, C. A. Meegan, J. van Paradijs, G. J. Fishman, N. P. Bhat, M. S. Briggs, T. M. Koshut, W. S. Paciesas, & G. N. Pendleton, *ApJ* **413** (1993) L101.

[3] E. Nakar, & T. Piran, *MNRAS* **360** (2005) L73.

[4] D. L. Band & R. D. Preece, *ApJ* **627** (2005) 319.

[5] L. Amati, et al., *A&A* **390** (2002) 81.

[6] G. Ghirlanda, G. Ghisellini, & D. Lazzati *ApJ* **616** (2004) 331.

[7] D. A. Frail, *ApJ* **562** (2001) L55.

[8] E. Nakar, *Physics Reports* **442** (2007) 166.

[9] D. Watson, et al., *A&A* **454** (2006) L123.